Technetium-99m-Antiepidermal Growth Factor-Receptor Antibody in Patients with Tumors of Epithelial Origin: Part II. Pharmacokinetics and Clearances

Normando Iznaga-Escobar, Leonel A. Torres Arocha, Alejo Morales Morales, Mayra Ramos Suzarte, Nelson Rodríguez Mesa and Rolando Pérez Rodríguez

Center of Molecular Immunology, Center of Clinical Researches, and Medical Surgical-Research Center, Havana, Cuba

Radiolabeled antitumor antibodies hold promise for diagnostic imaging and therapy in oncology. The purpose of this study was to investigate the pharmacokinetics, clearances and possible differences of two dosage administrations of the ^{99m}Tc-labeled antiepidermal growth factor (EGF)-receptor antibody and to predict the best dose and schedule for future clinical evaluations of this radiopharmaceutical. **Methods:** Nine patients (4 women, 5 men; mean age 46.4 ± 14.0 yr) were administered 1–3 mg ^{99m}Tc-labeled anti-EGF-receptor antibody (a murine IgG$_{2a}$ isotype) by intravenous bolus infusion. After administration, blood samples were collected from 7 patients from an antecubital vein opposite to the injection side at intervals from 2 min to 24 hr after injection, and plasma samples were obtained for pharmacokinetic analysis. Appropriate plasma samples were examined for isotope clearance (i.e., μCi/ml at various intervals) and ^{99m}Tc complexation to plasma proteins by fast protein liquid chromatography (FPLC) analysis. Urine was collected from each patient at 3 hr intervals up to 24 hr after monoclonal antibody administration to monitor ^{99m}Tc clearance. Plasma time-activity curves were fitted to a two-compartment model using nonlinear least-squares regression analysis by the method of flexible polyhedrals. **Results:** Plasma disappearance curves of ^{99m}Tc-labeled anti-EGF-receptor antibody were best fit by biexponential equation with a distribution half-life (t$_{1/2\alpha}$) of 0.137 ± 0.076 hr (n = 7) and elimination half-life (t$_{1/2\beta}$) of 20.3 ± 8.0 hr. Analysis of urine showed that activity clearance by this route amounted to 4.9% ± 0.6% of the injected dose in 24 hr, and FPLC analysis showed no evidence of decomposition, only 6%–7% of ^{99m}Tc was in a low molecular weight species. **Conclusion:** Plasma pharmacokinetics and urine clearance indicate comparability in both doses. The pharmacokinetic properties of the ^{99m}Tc-labeled anti-EGF-receptor antibody were found to be dose-independent. These findings provide an initial characterization of the radiopharmaceutical disposition in patients and may be used as the basis for calculating a better estimate of biodistribution and dosimetry for patients who will receive ^{188}Re-labeled anti-EGF-receptor antibody (MAb ior egf/r3) injection for radioimmunotherapy and warrants further controlled clinical trials to define the efficacy of the radiopharmaceutical.
Key Words: antiepidermal growth factor receptor for antibody; radiolabeling; pharmacokinetics; plasma

J Nucl Med 1998; 39:1918–1927

The development of monoclonal antibodies (MAbs) with high affinity and high specificity for tumors has generated widespread interest in radiolabeled MAbs for radioimmunodiagnosis (RAID) and radioimmunotherapy of malignant solid tumors. Many reports on clinical investigations using radiolabeled antibodies for diagnosing malignant neoplasms have been published during the last few years (1–4). Although the

feasibility of imaging based on pharmacokinetic studies was established with MAbs labeled to long-lived radionuclides such as ^{131}I (1) and ^{111}In (5,6), improved imaging quality had been obtained using ^{99m}Tc (7). Most of these studies concentrated on imaging and evaluating the efficacy of radioimmunoscintigraphy. Also important, however, is determining pharmacokinetic parameters that may explain features in the images.

Some clinical studies have investigated pharmacokinetics by measuring blood activity clearance curves and the rate of urinary excretion of activity by quantitating activity levels in normal tissues, especially by the analysis of plasma samples to determine the chemical forms of the radioactivity present (8,9).

The human epidermal growth factor receptor (EGF-r) is a transmembrane glycoprotein of 1186 amino acids with a molecular weight of 170 KDa that contains an extracellular EGF-binding domain, a transmembrane domain and a cytoplasmic domain, which has tyrosine kinase activity and undergoes autophosphorylation on ligand binding (10,11). EGF-r overexpression has been found in a variety of malignant epithelial tumors arising in different organs like the breast (12,13), bladder (14), colon (15) or lung (6,16) and in gliomas (17).

The MAb ior egf/r3 developed at the Center of Molecular Immunology, Havana, Cuba is a murine IgG$_{2a}$ antibody that recognizes the EGF-r. Its properties have been described previously (18,19). When bound to the membrane-receptor complex, it becomes internalized with the receptor causing down regulation of the EGF-r without stimulating tyrosine kinase activity. These characteristics have been used widely in the RAID of tumors of epithelial origin. The MAb ior egf/r3 was shown valuable for detecting occult epidermoid carcinoma cells in patients with lung tumors, breast tumors and gliomas (20).

We report the human pharmacokinetics and clearances of the ^{99m}Tc-labeled anti-EGF-r antibody (ior egf/r3) in patients with tumors of epithelial origin.

MATERIALS AND METHODS

Patients

Nine patients with tumors of epithelial origin were selected from ongoing Center for Medical-Surgical Researches (CIMEQ, Havana, Cuba) Phase I/II protocols. The study was approved by the ethics committee of the CIMEQ Hospital and by the National Regulatory Authorities of Cuba, the Center for State Control of Quality of Drugs (CECMED, Havana, Cuba). Technetium-99m-labeled mAb ior egf/r3 was administered to 9 patients (4 women, 5 men; age range 19–64 yr; mean age 46.4 ± 14.0 yr) for pharmacokinetic studies. Table 1 provides demographic information and the anatomical locations of the tumors. Written informed consent was obtained from all patients entered in the study.

TABLE 1
Patient Data

Patient no.	Age (yr)	Sex	Weight (kg)	Height (cm)	Diagnosis
1	54	F	50	157.5	Lung cancer
2	19	F	44.5	164	Glioblastoma multiforme
3	33	F	61	156	Suspected glioblastoma
4	42	M	81.5	171	Resected hypernephroma with brain metastases
5	51	M	77	182	Lung cancer with bone metastases
6	42	F	52	154	Lung cancer, Stage III
7	64	M	58.5	163.5	Lung cancer, Stage IIIb
8	56	M	62	167	Lung cancer
9	57	M	84.5	174	Lung neoplasm with hepatomegaly
Mean ± s.d.	46.4 ± 14.0	—	63.4 ± 14.4	165.4 ± 9.2	—

Monoclonal Antibody

The MAb ior egf/r3 is a highly specific murine IgG_{2a} isotype antibody that recognizes EGF-r. The MAb ior egf/r3 is secreted by hybridoma A24/15/128 obtained by fusion of murine myeloma cells SP2/Ag14 with splenocytes from Balb/c mice immunized with a partial purified fraction of the human EGF-r from human placenta. Its generation, characterization and reactivities have been described in detail previously (18,19). Vials containing 1 ml sterile and apyrogenic neutral solution with an antibody concentration of 5 mg/ml were used.

Reduction of Antibody, Radiolabeling and Quality Control

The antibody, concentrated to 5 mg/ml by ultrafiltration with a Centricon-30 (Amicon, Bedford, MA) in neutral phosphate-buffered saline (PBS), was reduced by reaction with a molar excess of 2-mercaptoethanol (2-ME) of 2000:1 (2-ME to Ab) at room temperature for 30 min. The reduced antibody was purified to eliminate the excess of 2-ME on a Parkinson's disease-10 Sephadex G-25 M gel filtration column (Pharmacia Biotech, Uppsala, Sweden) using cold phosphate-buffered saline (pH 7.4) purged with nitrogen as mobile phase. A fraction of 2 ml was collected and protein concentration determined measuring the OD at 280 nm on an ultraviolet/visible spectrophotometer (Pharmacia Biotech).

The ability of the reduced MAb to label with ^{99m}Tc was assessed, as described previously (21). Briefly, aliquots of 1 and 3 mg/ml of reduced antibody were used. After reduction of intrinsic disulfide bonds, the Amerscan Medronate II bone-scanning kit (Amersham, London, United Kingdom) was reconstituted with 5 ml 0.9% sodium chloride purged with nitrogen, and 50 μl/mg antibody of this solution were added to the reduced MAb and they were labeled with 50 mCi pertechnetate (TcO_4^-) eluted from the $(^{99}Mo/^{99m}Tc)$ generator (Amersham). The specific activity obtained was about 50 mCi/mg antibody. Activity was measured in a Compucal II (Nuclear Associates, Division of Victoreen Inc., London, United Kingdom) radioisotope dose calibrator.

The labeled product was subjected to ascending paper chromatography on Whatmann 3MM paper as stationary phase and 0.9% saline and acetone as mobile phase. Radioactivity bound to antibody remained at the origin, whereas free pertechnetate and ^{99m}Tc-methylene diphosphonate (MDP) migrated with the solvent front (21).

Human serum albumin (1%)-impregnated instant thin-layer chromatography-silica gel (Gelman Science Inc., Ann Arbor, MI) strips were used as stationary phase and ethanol:NH_4OH:water (2:1:5 v/v) as the mobile phase to separate radiocolloids that remained at the base while the radiolabeled MAb and free pertechnetate moved away (colloid, $R_f = 0.0$; labeled ^{99m}Tc, $R_f = 1.0$) (22).

Antibody Immunoreactivity

Immunoreactivity of the reduced antibody was performed by homogeneous radioreceptor analysis (RRA) (23), measuring its ability to interact with the EGF-r expressed in a human placenta microsomal fraction. Reduced antibody was compared with non-reduced (native) antibody for the ability to compete with radioiodinated murine EGF (^{125}I-EGF). Different concentrations of antibody (reduced and nonreduced) were used. Data from three to five independent experiments were averaged, plotted and subjected to an exponential fit, and the concentration for each antibody preparation that produced half-displacement (50% inhibition) of labeled EGF was estimated from the fitted curves.

Radiopharmaceutical Administration

Five patients were administered 30.3 ± 11.9 mCi (mean ± s.d.) (1 mg MAb) and four were given a dose of 39.5 ± 1.1 mCi (3 mg MAb) by intravenous bolus infusion through a peripheral vein. The appropriate dose was measured by a radioactivity calibration system (Compucal II, Nuclear Associates). No adverse reactions were noticed in any of the patients during or after the infusion.

Blood and Urine collection

After intravenous injection, 3- to 4-ml blood samples were collected in seven patients from an antecubital vein opposite the injection side at timed intervals (2, 5, 10, 20 and 30 min and 1, 3, 5, 8, 18 and 24 hr postinjection), and 1-ml aliquots of whole, anticoagulated blood with heparin were immediately centrifuged (5 min, 3000 rpm) at room temperature and plasma was removed with an eppendorf pipette.

Urine was collected from each patient at 3-hr intervals up to 24 hr postinjection, and the total volume of each collection was recorded.

The radioactivity in plasma and urine (0.3-ml aliquots) samples was determined in duplicate by counting in a fixed, reproducible geometry system gamma counter (Scaler Ratemeter SR8; Nuclear Enterprise, London, United Kingdom) to obtain the total counts. All samples were counted for 10 sec, which generally provided a counting error of less than 1%, except for those samples from the later collection periods that contained very low levels of radioactivity. The total counts of radioactivity in plasma and urine samples were then converted to activity concentration in μCi/ml, using a standard prepared at the time of the injection. Appropriate corrections were made for decay using the time of injection as the reference time.

Pharmacokinetic Data Analysis

Plasma activity concentration in μCi/ml was multiplied by total plasma volume of each patient to obtain whole plasma activity. Thereafter, plasma activity was expressed as the fraction of administered activity remaining in plasma at each counting time and related to the total percentage injected dose (%ID). The pharmacokinetic plasma data were analyzed using model-dependent analyses performed according to Akaike's information criteria (AIC) (24) as a statistical test by a software package (BRASIER, provided by the High Institute of Nuclear Sciences and Technology

[ISCTN], Havana, Cuba) that performs nonlinear least-squares regression analysis using the flexible polyhedrals method (25). For model-dependent analyses, the best estimates were obtained by fitting a biexponential model to the plasma activity versus time data using:

$$C(t) = A_1 e^{-\lambda_1 t} + A_2 e^{-\lambda_2 t} \qquad \text{Eq. 1}$$

where C (t) is the plasma activity in $\mu Ci/ml$ of ^{99m}Tc-ior egf/r3 at time t, A_1 and A_2 are the activity concentration constants for the first and second phases, respectively, and λ_1 and λ_2 are the first-order rate constants for respective phases.

The first and second phase half-lives ($T_{1/2}$) were calculated from standard pharmacokinetics equations using the first-order rate constants, i.e.:

$$t_{1/2\alpha} = \ln(2)/\lambda_1 \text{ and } t_{1/2\beta} = \ln(2)/\lambda_2 \qquad \text{Eq. 2}$$

The parameters derived from the biexponential fit were used to calculate model-dependent pharmacokinetic parameters as previously described (26–28). The area under the time-activity curve (AUC) is equal to the sum of the areas under each exponent and was determined using:

$$AUC = A_1/\lambda_1 + A_2/\lambda_2 \qquad \text{Eq. 3}$$

the area under the moment curve was calculated using:

$$AUMC = A_1/\lambda_1^2 + A_2/\lambda_2^2 \qquad \text{Eq. 4}$$

and the maximal activity concentration by:

$$C_0 = A_1 + A_2 \qquad \text{Eq. 5}$$

The other pharmacokinetic parameters, apparent volume of the central compartment (V_c), apparent volume of distribution at steady state (V_{ss}) and apparent volume of distribution of peripheral tissue (V_t), were calculated according to standard methods (29).

The mean residence time in the central compartment (MRT_c), mean residence time in peripheral tissues (MRT_p) and the mean residence time in the body (MRT_b) were calculated according to Webster et al. (30).

Clearance and Excretion Studies

Total-body clearance (CL_D) was calculated using:

$$CL_D = Dose/AUC \qquad \text{Eq. 6}$$

and the elimination from systemic circulation can be described by fraction of dose renally cleared (CL_R) using:

$$CL_R = A_R/AUC \qquad \text{Eq. 7}$$

where A_R is the cumulative amount of total radiopharmaceutical excreted unchanged from the time of dosing to the end of the last void interval and AUC represents the area under the total radiopharmaceutical plasma time-activity profile during this period (31). The fraction of dose cleared nonrenally (CL_{NR}) can be calculated by:

$$CL_{NR} = CL_D - CL_R \qquad \text{Eq. 8}$$

where CL_{NR} represents the fraction of dose cleared by organs other than the kidneys.

Fast Protein Liquid Chromatography Analysis

Fast protein liquid chromatography (FPLC) analysis also was performed on plasma samples to measure the percentage of ^{99m}Tc transcomplexed to plasma proteins and to analyze molecular composition. Plasma samples of 200 μl obtained at 1 and 5 hr postinjection were applied to a Pharmacia system (Pharmacia Biotech; Uppsala, Sweden) equipped with a Superose 12 high-

resolution 10/30 size exclusion column eluted at a flow rate of 0.5 ml/min with 0.1 M phosphate buffer (pH 7.4). Fractions of 500 μl were collected, and the activity in the plastic tubes used for protein analysis and measurement of gamma radiation in a gamma counter was analyzed.

Patient Imaging

Whole-body scans were performed on a Sophy DS-7 (Sopha Medical Systems, Ottawa, Canada) gamma camera, fitted with a low-energy high-resolution, diverging parallel-hole collimator to increase the lateral viewing aspect. Images were acquired using a 20% window centered on the 140 keV emission from ^{99m}Tc after injection. Anterior and posterior whole-body scans were acquired at 5 min, 1, 3, 5 and 24 hr postinjection using a gantry speed of 20 cm/min; acquisition times were approximately 25 min each. All whole-body images were stored on the computer in a 2048 $\times$ 512 matrix. The geometric mean of anterior and posterior images corrected for decay was obtained, and regions of interest (ROIs) were drawn over the organs that took up enough radioactivity to be visualized on the images and, therefore, were considered as the source organs. In some cases, a framework was extracted from the geometric mean of anterior and posterior views.

Statistical Analysis

To calculate plasma pharmacokinetic parameters, data were entered into a statistical program that yielded biexponential fits with a correlation coefficient greater than 0.9901, and the model was selected according to the AIC (24) as a statistical test. Data were analyzed to give group mean values and standard deviation. Statistical significance of differences between pharmacokinetic parameters for the 1- and 3-mg doses was determined by the software MicroCal Origin Version 3.0 (MicroCal Software, Inc., Northampton, MA) using two-tailed Student's t-test for unpaired data, when appropriate, with $p > 0.05$ being considered significant.

RESULTS

Radiolabeling

All radiolabeled procedures were performed under aseptic conditions in a shielded laminar flow hood. All glassware, plastics and solutions were sterile and pyrogen free. For labeling the MAb ior egf/r3, IgG_{2a} with ^{99m}Tc, the procedure described in the Materials and Methods section was followed. The purified MAb ior egf/r3 was labeled with a specific activity of 50 mCi/mg protein. A mean of 98.8% $\pm$ 1.2% ^{99m}Tc was bound to IgG_{2a}, as determined by paper chromatography. Instant paper chromatography of labeled MAb in acetone showed about 1.2% or less free pertechnetate ran at the solvent front ($R_f = 1.0$). This indicates that pertechnetate was reduced almost quantitatively. When the chromatogram was developed in saline, more than 98.8% of the activity stayed at the origin, indicating that the ^{99m}Tc was transchelated from MDP to the MAb ior egf/r3. As a rule, the colloid formation, determined by albumin-impregnated ITLC was < 1.5% in all preparations.

Antibody Immunoreactivity

The immunoreactivity of the reduced MAb was assessed using an RRA, as described in the Materials and Methods section. Nonreduced (native) and reduced MAbs ior egf/r3 were tested for their ability to compete with radioiodinated EGF for the binding to EGF-r in the human placental extract. The reduced and native antibodies were able to compete completely with radioiodinated EGF for the binding to EGF-r at similar protein concentrations (Fig. 1). As determined by this RRA, the concentration for native and reduced antibodies that inhibit the binding of radioiodinated EGF to its receptor at 50% were 0.586 $\pm$ 0.073 $\mu g/ml$ and 0.731 $\pm$ 0.068 $\mu g/ml$ for both
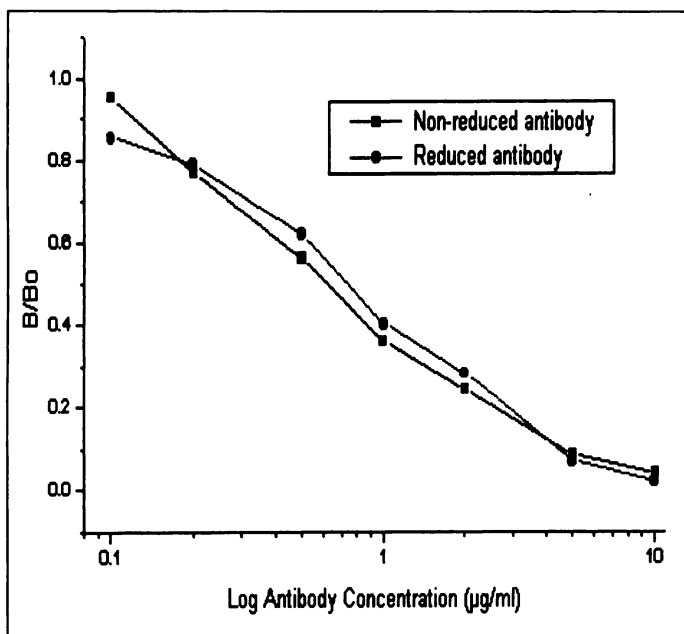
FIGURE 1. Immunoreactivity of MAb ior egf/r3 analyzed by RRA. Reduced (●) MAb ior egf/r3 was compared with nonreduced (native) MAb ior egf/r3 standard (■), as described in Materials and Methods section.

preparations, respectively. There were no statistically significant differences between values (p < 0.05) by Student's t-test.

Pharmacokinetics

Pharmacokinetic parameters were obtained for seven patients. The percentage of circulating radioactivity on formed elements was determined from blood samples in five patients. Approximately 98% ± 2% of radioactivity in whole blood was found in the plasma fraction at all times. No significant binding of the antibody to circulating blood cells was observed. The radioactivity content of plasma expressed as %ID was plotted against the time of blood drawing in a log plot (Fig. 2). Plasma time-activity curves were best adequately fit to a biexponential equation with a correlation coefficient of 0.99 ± 0.01 and with a distribution half-life $(t_{1/2\alpha})$ of 0.137 ± 0.076 hr (range

0.062–0.246 hr; n = 7) and elimination half-life $(t_{1/2\beta})$ of 20.3 ± 8.0 hr (range 12.6–33.9 hr), respectively (Table 2). The statistical difference between mean value for pharmacokinetic parameters for each dose was calculated by two-tailed, unpaired Student's t-test. The significant differences between mean values of half-lives for 1- and 3-mg doses evaluated by Student's t-test are indicated by an asterisk in Table 2, corresponding to p < 0.01. There were no significant differences at the p < 0.05 level for the other pharmacokinetic parameters in both doses, as expected. The AUC was 69.8 ± 57.3 μCi/ml × hr, and the maximal activity concentration was 8.3 ± 3.1 μCi/ml.

Results for mean residence times for ^{99m}Tc-labeled MAb ior egf/r3 in the seven patients studied are shown in Table 3. MRT_c was 6.6 ± 4.1 hr and significative differences between both doses were found at p < 0.05. MRT_p was 22.5 ± 9.4 hr, and MRT_b was 29.2 ± 13.2 hr.

Results for apparent volumes of distribution are shown in Table 4. The mean V_c was 65.7 ± 26.2 ml/kg, mean V_{ss} was 385.9 ± 293.7 ml/kg and V_t was 320.3 ± 272.5 ml/kg.

Clearance and Urine Excretion

Data on the plasma and urine elimination after intravenous injection were analyzed with a pharmacokinetic model. Systemic clearance of ^{99m}Tc-labeled MAb ior egf/r3 was determined in seven patients. CL_D was 17.7 ± 22.4 ml/hr/kg (range 2.87–65.16 ml/hr/kg) (Table 5).

The analysis of urinary excretion data of ^{99m}Tc-labeled MAb ior egf/r3 was evaluated in all patients, and the activity excreted in microcuries was plotted against the time interval (Fig. 3). The urinary bladder time-activity curves were typically sawtooth-shaped curves and were described using a semidynamic bladder model. The cumulative activity, A_R (AUC), was obtained by integrating the Equation 7 for each interval from 0 to the last void point. The analysis revealed a CL_R of ^{99m}Tc-labeled MAb ior egf/r3 of only 0.87 ± 1.19 ml/kg (range 0.15–3.45 ml/kg), and the 0–24-hr cumulative urinary excretion data (Table 5) for seven patients indicated that the renal excretion was not the major elimination route for ^{99m}Tc-labeled MAb ior egf/r3 with 4.9 ± 0.6% ID (range 4.1–5.9% ID) being excreted within 24 hr
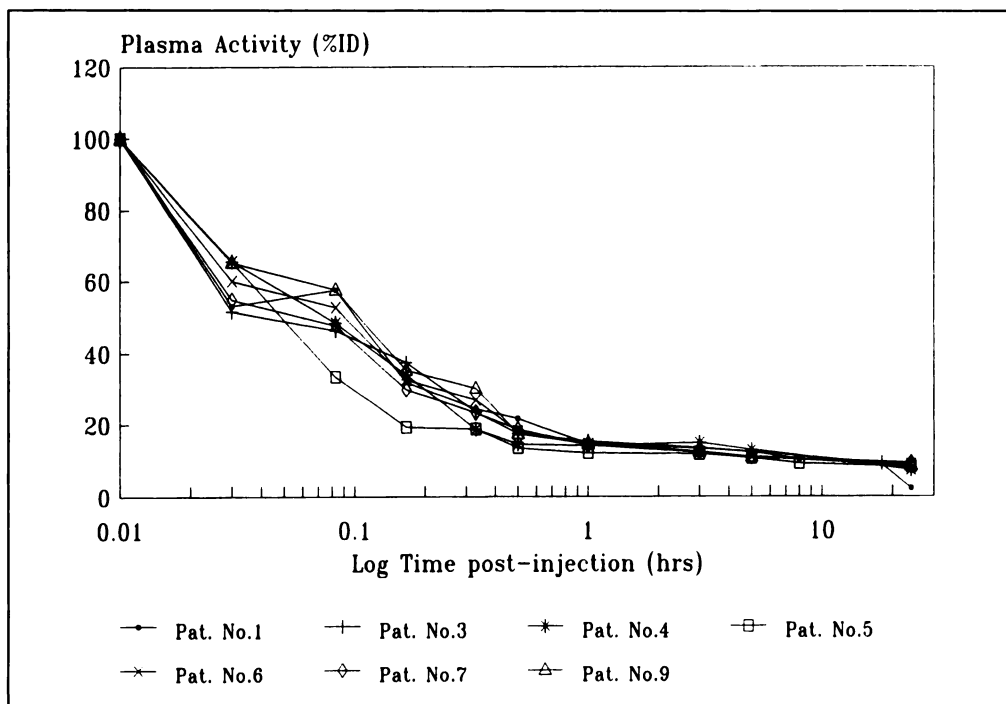
FIGURE 2. Plasma disappearance curves of ^{99m}Tc-labeled MAb ior egf/r3 in log plot. The solid lines represent best-fit curves of biexponential data, with correlation coefficient of 0.99 ± 0.01 determined by nonlinear least-squares regression, using method of flexible polyhedrals.

TABLE 2
Pharmacokinetic Parameters

| Patient no. | Administered dose | | Distribution | Elimination | Co | AUC |
	mg	mCi	$t_{1/2\alpha}$ (hr)*	$t_{1/2\beta}$ (hr)[†]	(μCi/ml)[†]	(μCi/ml $\times$ hr)[†]
1	1	39.2	0.062	16.4	12.2	114.02
3	1	41.9	0.118	26.1	11.1	171.04
4	1	20.4	0.087	33.9	5.3	87.15
5	1	19.7	0.071	24.1	3.6	40.78
Mean ± s.d.	1	30.3 ± 11.9	0.085 ± 0.025	25.1 ± 7.2	8.1 ± 4.2	103.25 ± 54.39
6	3	38.5	0.235	12.7	6.9	11.37
7	3	39.3	0.139	16.4	9.9	25.48
9	3	40.7	0.246	12.6	8.8	38.73
Mean ± s.d.	3	39.5 ± 1.1	0.207 ± 0.059	13.9 ± 2.2	8.5 ± 1.5	25.19 ± 13.68
Mean ± s.d.	—	34.2 ± 9.8	0.137 ± 0.076	20.3 ± 8.0	8.3 ± 3.1	69.8 ± 57.3

*Significant differences between doses were found at $p < 0.01$.
[†]No statistical differences between doses were found at $p < 0.05$.
Co = activity concentration; AUC = area under the time-activity curve.

of radiopharmaceutical administration under physiological conditions. The 0–24-hr urinary excretion of ^{99m}Tc-labeled MAb ior egf/r3 did not correlate linearly with the dose administered ($r = 0.39$, $p < 0.05$), and these values did not differ with the dose of the labeled MAb injected.

Fast Protein Liquid Chromatography Analysis

The 1- and 5-hr plasma samples were passed over a Superose 12 high-resolution 10/30 FPLC size-exclusion column to determine the molecular composition of the product remaining in the plasma. A single radioactive peak was observed that was identical to the ultraviolet absorbance peak at 10.4 min retention time, which corresponded to ior egf/r3 MAb. The results of the analysis of the samples taken 1 and 5 hr after injection showed no evidence of complexation or appreciable breakdown of the labeled antibody to free pertechnetate and suggested that the bulk of the radioactivity still was associated with the MAb fraction and that a small amount of ^{99m}Tc was present in a low molecular weight species even after 5 hr of the injected dose (Fig. 4), as evidenced by a peak in the 26 fraction where the technetium content in a low molecular weight species of <7%.

The recovery of the protein concentration associated with the radioactivity in the mean peak of the chromatogram was >95%.

Imaging

Multiple images were obtained in nine patients. Whole-body images up to 24 hr postinjection showed decreasing blood-pool activity during the first hours, with the liver, heart and spleen visualized. Uptake of activity also was seen sometimes in the intestine and in the urinary bladder at later times. No selective accumulation of radioactivity was observed in any other normal tissue. For 1- and 3-mg doses, the antibody was rapidly removed; only 12.9% ± 1.1% of the injected activity was circulating in the blood 3 hr after the end of administration. At that time, there was a large concentration in the spleen and liver. The presence of EGF-r in the liver cells contributed to the rapid removal of labeled MAb from blood. Figure 5 shows a geometric mean of the anterior and posterior whole-body images obtained at 1, 3, 5 and 24 hr postinjection and illustrates the normal biodistribution of ^{99m}Tc-labeled MAb ior egf/r3. These images are typical of those obtained in patients thought to be disease free, and they showed early and persistent high-

TABLE 3
Mean Residence Times

Patient no.	MRT$_c$ (hr)*	MRT$_p$ (hr)[†]	MRT$_b$ (hr)[†]
1	5.5	17.7	23.2
3	12.5	32.0	44.6
4	10.1	37.2	47.3
5	9.7	25.7	35.3
Mean ± s.d.	9.5 ± 2.9	28.2 ± 8.4	37.6 ± 10.9
6	1.7	13.2	14.9
7	2.6	19.4	21.9
9	4.4	12.6	17.0
Mean ± s.d.	2.9 ± 1.4	15.1 ± 3.7	17.9 ± 3.6
Mean ± s.d.	6.6 ± 4.1	22.5 ± 9.4	29.2 ± 13.2

*Significant differences were found at $p < 0.05$.
[†]No statistical differences were found at $p < 0.05$.
MRT$_c$ = mean residence time in central compartment; MRT$_p$ = mean residence time in peripheral tissues; MRT$_b$ = mean residence time in body.

TABLE 4
Apparent Volumes of Distribution

Patient no.	V_c (ml/kg)*	V_{ss} (ml/kg)*	V_t (ml/kg)*
1	37.9	159.6	121.7
3	50.3	218.9	168.6
4	46.6	218.8	172.2
5	94.3	344.2	249.9
Mean ± s.d.	57.3 ± 25.2	235.4 ± 77.7	178.1 ± 53.1
6	108.2	970.3	862.1
7	67.9	578.2	510.3
9	54.6	211.6	157.0
Mean ± s.d.	76.9 ± 27.9	586.7 ± 379.4	509.8 ± 352.5
Mean ± s.d.	65.7 ± 26.2	385.9 ± 293.7	320.3 ± 272.5

*No statistical differences were found at $p < 0.05$.

V_c = apparent volume of central compartment; V_{ss} = apparent volume of distribution at steady state; V_t = apparent volume of distribution of peripheral tissue.

activity levels in liver and spleen. A good clearance was seen at 24 hr for both organs. In the 1-hr image, some activity is prominent in blood pool that decreased such that at 24 hr blood vessels are barely discernible. At 24 hr, some bowel radioactivity, probably due to hepatobiliary excretion can be seen, indicating that the bowel is one of the major sites of excretion. Figure 6 is of a patient with primary, Stage III lung cancer in which a metastasis in the lymphatic nodules of the laryngeal region was detected by immunoscintigraphy and confirmed by biopsy. Serial imaging performed at 5 min and 1, 3 and 5 hr showed increased laryngeal region uptake is shown inside the circles (Fig. 6). The specific tumor metastasis uptake seen for ^{99m}Tc-labeled MAb ior egf/r3 was due to the high specificity and good internalization properties of this MAb. After binding to the receptor, the ^{99m}Tc-labeled MAb ior egf/r3-EGF-r complex is rapidly internalized and the complex is translocated from the cytoplasm to the nucleus of the cells. Figure 7 is a 3-hr anterior scan of the chest of Patient 9, a 57-yr-old man with a primary lung neoplasm with hepatomegaly, showing metastases with an area of increased ^{99m}Tc-labeled MAb ior egf/r3 activity (circles) in the right anterior pectoral area.

DISCUSSION

Recently, many researchers have become aware of the need to investigate the pharmacokinetics and clearances of MAbs in humans in greater detail to understand how these are related to such factors as variability in tumor size and number of binding sites among patients, MAb specificity and binding avidity, immunoreactivity, MAb internalization after binding, immunogenicity, MAb dose and the type of radioisotopes (32). These factors contribute to the difficult and poorly understood pharmacokinetics of radiolabeled MAbs. The number of available antigen binding sites will alter MAb pharmacokinetics and biodistribution. Divgi et al. (6) and Halpern and Hagan (33) have demonstrated changes in serum clearance rates with an increased antibody dose. Carrasquillo et al. (34) failed to detect any changes in antibody clearance after preloading experiments with unlabeled antibody, and several clinical trials have reported a range of antibody doses were used. Iodine-131-B72.3 antibody was used at doses of 0.27, 1.19 and 3.8 mg, and no significant differences in blood clearances or in tumor uptake were reported (35) and no dose-dependent tumor uptake for ^{111}In-T101 was seen in cutaneous T-cell lymphoma using doses

TABLE 5
Clearances and Urine Excretion

Patient no.	CL_D (ml/hr/kg)*	CL_R (ml/kg)*	CL_{NR} (ml/hr/kg)*	Total urine excretion in 24 hr (%)
1	6.88	0.31	6.87	4.5
3	4.02	0.22	4.01	5.9
4	2.87	0.15	2.86	5.1
5	6.27	0.30	6.26	4.7
Mean ± s.d.	5.01 ± 1.88	0.25 ± 0.08	5.00 ± 1.88	5.05 ± 0.62
6	65.16	3.45	65.0	5.3
7	26.51	1.16	26.5	4.4
9	12.44	0.51	12.4	4.1
Mean ± s.d.	34.7 ± 27.3	1.71 ± 1.54	34.6 ± 27.2	4.6 ± 0.6
Mean ± s.d.	17.7 ± 22.4	0.87 ± 1.19	17.7 ± 22.4	4.9 ± 0.6

*No statistical differences were found at $p < 0.05$.

CL_D = total-body clearance; CL_R = renal clearance; CL_{NR} = nonrenal clearance.
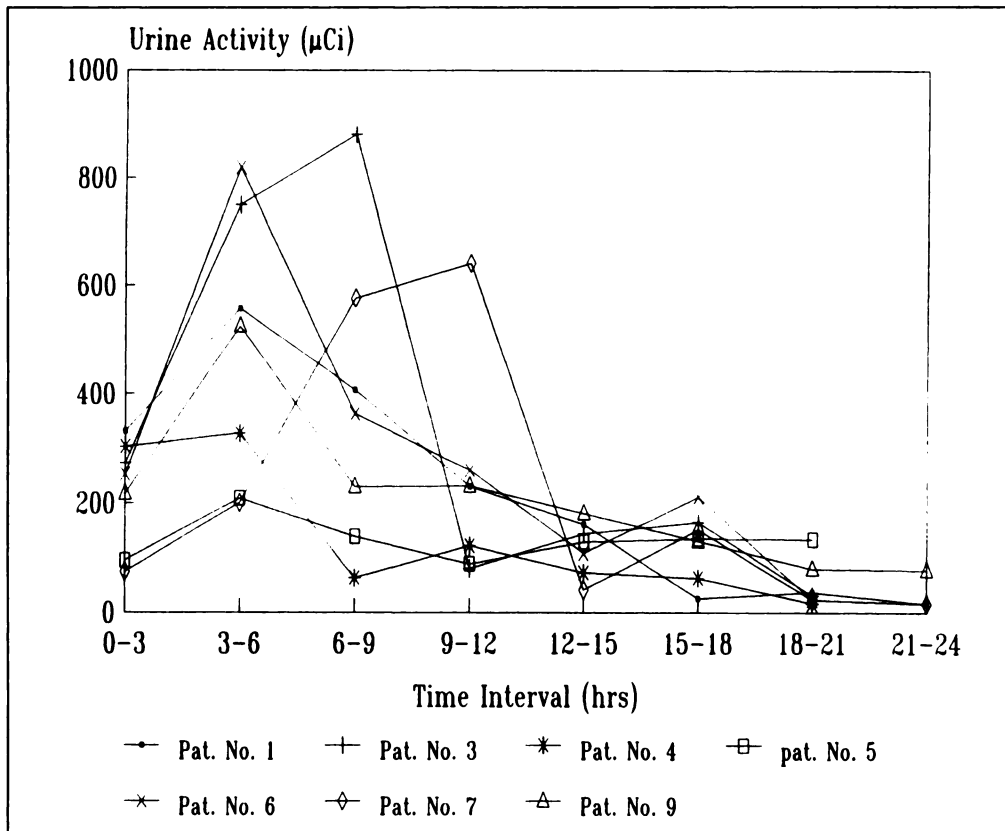
FIGURE 3. Urinary excretion patterns of ^{99m}Tc-labeled MAb ior egf/r3 in seven patients receiving intravenous bolus injection. Urinary excretion patterns are essentially identical.

of 1–50 mg (36). De Bree et al. (37), using ^{99m}Tc-labeled MAb U36 at doses of 2, 10 and 50 mg, also demonstrated that an increase in the MAb dose did not influence clearance from blood or tumor uptake. In contrast, an increased number of sites of metastases of malignant melanoma were detected when the dose of ^{111}In-ZME-018 was increased from 2.5 to 10 mg (38). Therefore, a general statement on the dose-response relationship for all antibody-tumor combinations cannot be made. It is likely that higher doses of antibody may be required when levels of circulating antigens or antigen expressed in normal tissues are significant, as occurred in our case, in which each liver cell expresses about 105 binding sites, although conflicting reports exist in the literature (39). The area of antibody

metabolism is poorly understood and needs intense investigation if the best use of these materials is to be made. In general, an enhanced ability to detect lesions has been noted with an increasing antibody dose in earlier studies (6,40–42) and in this study. The assumed mechanism of the described findings is an increased saturation of antibody binding in the liver with increasing administered dose, leading to decreased plasma clearance and greater availability of antibody to target antigen in the tumor. The effect of dose on relative hepatic activity differs in various tumor systems, possibly due to a variable contribution of blood-pool activity to total hepatic activity.

During the past 15 yr, several mouse MAbs have been raised against epitopes on the external domain of the EGF-r and these
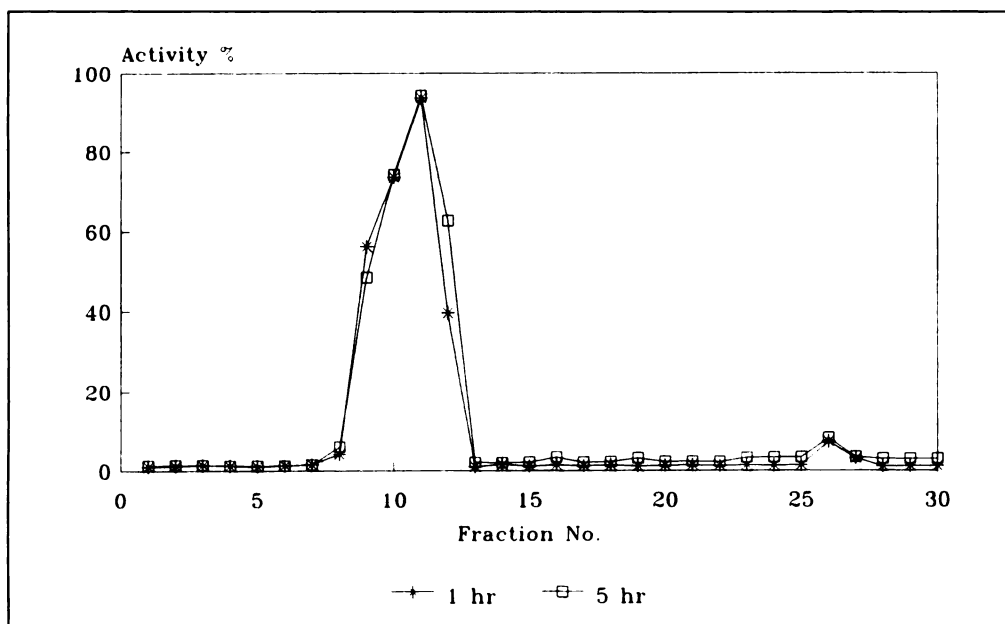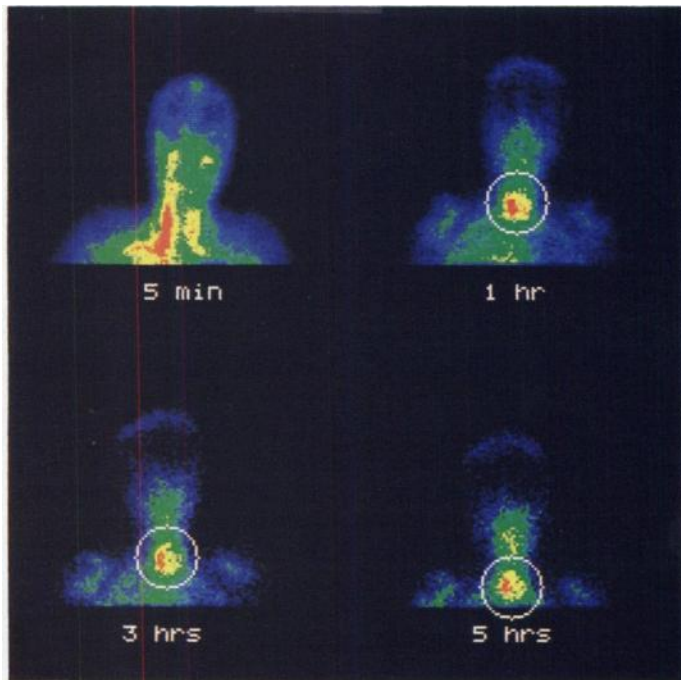

FIGURE 4. Representative 1- and 5-hr postinjection plasma profile (Patient 6). Largest peak represents ^{99m}Tc-labeled MAb ior egf/r3 and last peak illustrates 6%–7% of ^{99m}Tc in low molecular weight species.
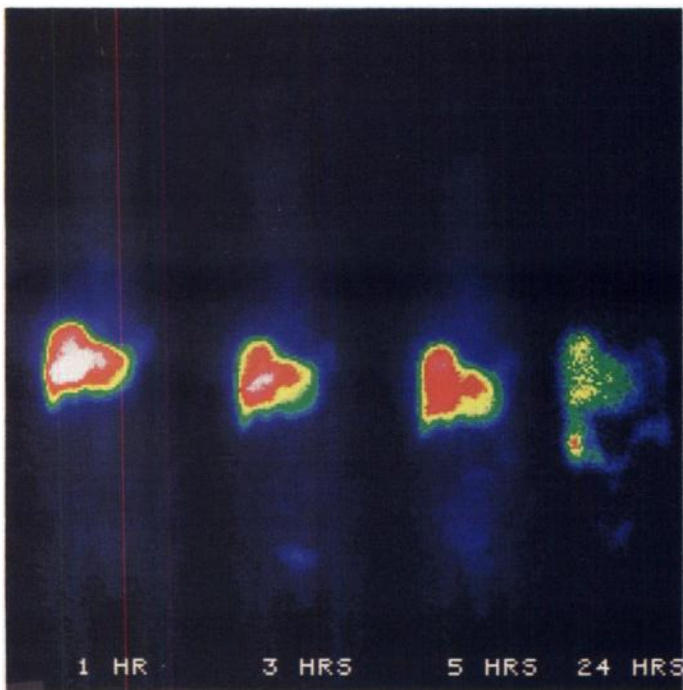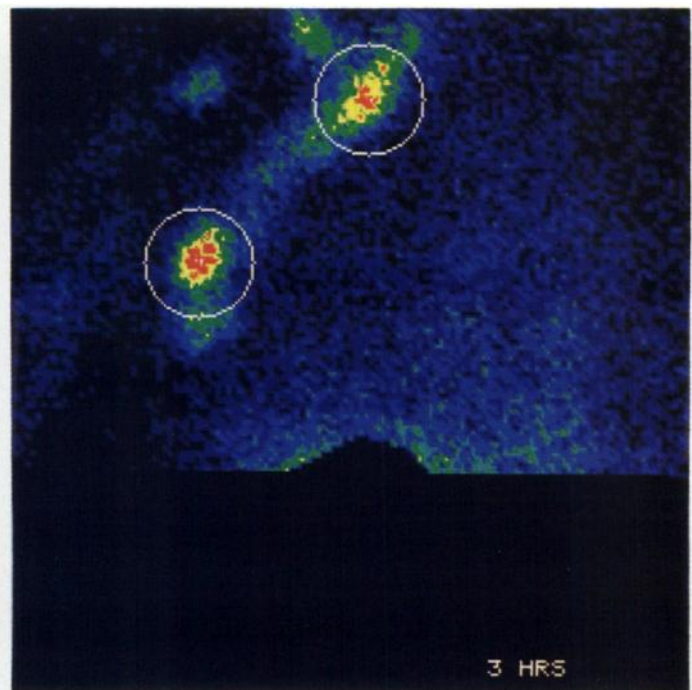
FIGURE 5. Serial whole-body images of Patient 8 obtained at 1, 3, 5, and 24 hr after injection show normal body distribution of radioimmunoconjugate, with early accumulation of radioactivity in spleen and liver and with rapid clearance at 24 hr through bowel and urinary bladder.

FIGURE 7. Anterior scan of chest at 3 hr of Patient 9, a 57-yr-old man with primary lung neoplasm with hepatomegaly, shows metastatic region with area of increased ^{99m}Tc-labeled MAb ior egf/r3 activity (circles) in right anterior pectoral area.

have been to investigate growth factor–receptor interaction and for radioimmunodiagnostic and radioimmunotherapeutic applications in cancer (43–48).

We described here the pharmacokinetic parameters of ^{99m}Tc-labeled MAb ior egf/r3 in patients with tumors of epithelial origin. The quality-control studies showed good incorporation of ^{99m}Tc onto the MAb ior egf/r3, excellent immunoreactivity and stability of the MAb in vivo, with only a small amount of the ^{99m}Tc in a low molecular weight species.

FIGURE 6. Serial images of anterior chest of Patient 6, a 42-yr-old woman with Stage III primary lung cancer that had metastasized to lymphatic nodules in laryngeal region. Initial images obtained at 5 min and 1, 3 and 5 hr show increasing uptake with time in lymph nodes of laryngeal region.

In human clinical trials, ^{99m}Tc-labeled MAb ior egf/r3 has been administered intravenously as a bolus injection to cancer patients to predict the best dosage and schedule for future clinical evaluations of this radiopharmaceutical, the fundamental pharmacokinetic parameters and the possible differences between 1- and 3-mg dose administration.

Least-squares regression using the method of flexible polyhedrals adequately fit our experimental data with the correlation coefficient of 0.99 ± 0.01 and provides estimates of the slopes and intercepts for the calculation of pharmacokinetic parameters. Pharmacokinetic analysis revealed that after intravenous bolus administration of ^{99m}Tc-labeled MAb ior egf/r3 the plasma disappearance curves for the seven patients could be described best by a two-compartment model, with a distribution half-life $t_{1/2\alpha}$ of 0.137 ± 0.076 hr and an elimination half-life $t_{1/2\beta}$ of 20.5 ± 8.0 hr (Table 2). These results agree with the pharmacokinetic parameters of unlabeled antibody measured by enzyme-linked immunosorbent assay (data not shown). The alpha and beta phase half-lives determined for ^{99m}Tc-labeled MAb ior egf/r3 were comparable with those reported in earlier studies in humans with ^{111}In-labeled MAbs (40) and with radioiodinated MAbs (41). In this study, 1 mg MAb was administered to five patients, who also showed a biexponential plasma profile with a rapid distribution phase resulting in the rapid removal of antibody from plasma within 2.1 ± 0.6 hr and 0.83 ± 0.13 hr followed by a more gradual elimination phase exhibiting a half-lives of 27 ± 8 hr and 31 ± 5 hr for both studies respectively.

Our results did not correlate with those obtained with MAb 225 (6), which demonstrated changes in serum clearances with increasing doses over a dosage range between 4 and 300 mg. In our studies, the shorter $t_{1/2\alpha}$ reflected the initial clearance from the central compartment and illustrated that ^{99m}Tc-labeled MAb ior egf/r3 was rapidly distributed to other compartments (tissues) outside the plasma. We believe this is due to rapid antibody-antigen binding between ^{99m}Tc-labeled MAb ior egf/r3 and the EGF-r. The relatively longer elimination half-life

reflects the retention of the radiopharmaceutical in the peripheral compartment (tumor and liver). These results agree with those obtained by Kirkwood et al. (42), who administered 2.5 mg to four patients, and the terminal half-life was about 19.6 ± 5.2 hr. As expected, no significant changes in half-lives were demonstrated at differing doses. Other individual differences seem to be responsible for variations of plasma disappearance, especially those related to tumor mass and tumor uptake of the antibody.

One advantage of the biexponential fitting to plasma profiles is that it allows the determination of mean residence times through the various compartments, which may furnish insights into the pharmacokinetics of the radiopharmaceutical that are not available otherwise. A comparison of MRT_c (6.6 ± 4.1 hr) (Table 3) with MRT_p (22.5 ± 9.4 hr) implies that ^{99m}Tc-labeled MAb ior egf/r3 resides inherently longer in the peripheral compartment (tissues) than in the central compartment (plasma). This finding would seem to be favorable for tumor targeting, because the tumor is likely to be situated in the peripheral compartment.

The apparent volumes of distribution, (Table 4) are similar to those reported by other investigators (49). The existence of more lesions (metastases) gives rise to a greater value of the V_{ss}, indicating extensive tissue binding of the radiopharmaceutical, which is further evidence that ^{99m}Tc-labeled MAb ior egf/r3 binds preferentially to tumors of epithelial origin that overexpress EGF-r and to metastatic lesions. V_t is consistent with antibody–antigen binding in the peripheral compartment, especially in tumors of epithelial origin and in the liver, because of the number of EGF-r present in those tissues and because the liver is the organ with the primary sites of excretion or metabolism of radiolabeled MAbs and their degradation products. No statistically significant (p < 0.05) differences in the pharmacokinetic measurement were seen in mean residence times and in the apparent volumes of distribution by two-tailed, unpaired Student's t-test. The reasons for this are the small number of subjects in each dose group and the large variances between individuals.

Plasma clearance for the 1- and 3-mg doses was rapid, with a mean retention of 12.9% ± 1.1% in the plasma at 3 hr postinjection and a mean of 7.4% ± 2.3% at 24 hr postinjection. ROI analysis from serial images showed a rapid clearance of radioactivity from the whole-body, liver and spleen (Fig. 5). In patients who received 1 and 3 mg MAb, there was rapid clearance of radioactivity into the liver and spleen 3 hr after injection, when 87% of the ^{99m}Tc-labeled MAb ior egf/r3 had been removed from circulation. The activity in the liver and spleen declined progressively, and a corresponding increase in uptake in the tumor was observed by 3 and 5 hr postinjection (Figs. 6 and 7). The rapid clearance from the whole body and from the major organs is faster than that observed for other ^{125}I- and ^{111}In-labeled MAbs targeted to solid tumors (45,46). Our results indicate that there is a reasonably high uptake of ^{99m}Tc-labeled MAb ior egf/r3 by tumors (Figs. 6 and 7) and satisfactory whole-body and blood clearances.

The elimination of radioactivity from plasma after administration of ^{99m}Tc-labeled MAb ior egf/r3 conjugate occurs primarily by metabolism of the immune conjugate and elimination of the radiolabeled MAb by renal and hepatobiliary excretion. No differences in clearances of ^{99m}Tc-labeled MAb ior egf/r3 were seen between the two dose levels. Because there was no technetium activity seen in the thyroid or stomach up to 24 hr postinjection in any of the patients (Fig. 5), the labeled product appears to be stable in vivo. This also is supported by the FPLC analysis of plasma samples obtained 1 and 5 hr after the administration of the radiopharmaceutical that showed less than 7% technetium in a low molecular weight species and more than 93% of the activity was MAb bound. The conclusion can be extrapolated to several hours postinjection when no breakdown of the labeled MAb is seen in urinary excretion, with only 4.9% ± 0.6% of the injected dose excreted after 24 hr. This conclusion is evident because plasma proteins such as albumin, transferrin and antibodies, among others, are too large to be filtered at the glomerulus and thus are retained in plasma (50).

The rapid targeting and clearance from plasma and normal organs of ^{99m}Tc-labeled MAb ior egf/r3 permitted the use of a short-lived radionuclide, such as ^{99m}Tc (6.02 hr), and confirmed that selective antibody accretion in tumors (Figs. 6 and 7) can occur very soon after administration. Imaging at 18–24 hr appeared to be optimum, although lesions could be detected as early as 3–4 hr postinjection.

Another issue that can affect plasma pharmacokinetics in humans would be an immunological response to murine antibodies (51), and the use of humanized antibodies (52) may eventually overcome problems caused by immune responses.

CONCLUSION

The plasma time-activity curves from seven patients showed a biexponential elimination that could be fitted adequately to a two-compartment model according to AIC as a statistical test. FPLC analysis of plasma samples up to 5 hr postinjection revealed that more than 93% of the radioactivity was bound to the MAb ior egf/r3.

Plasma pharmacokinetics and urine clearance indicate comparability of both doses. The pharmacokinetic properties of ^{99m}Tc-labeled MAb ior egf/r3 were found to be dose independent in our studies. The effect of administered dose on antibody half-life and biodistribution varies (53), depending on several factors. In our study, it might be due to: (a) the small range of dose used and the small number of subjects in each dose group; (b) the specific antibody-antigen system involved; and (c) possibly the radioisotope used (54). For intact MAb, our findings are consistent with many earlier studies of antibody pharmacokinetics using ^{125}I and ^{111}In (44–46). This study provides an initial characterization of radiopharmaceutical disposition in patients and may be used prospectively as the basis for calculating a better estimate of biodistribution and dosimetry for patients who will receive ^{188}Re-labeled MAb ior egf/r3 injection for radioimmunotherapy and warrants further controlled clinical trials to define its efficacy.

REFERENCES

1. Colcher D, Esteban JM, Carrasquillo JA, et al. Quantitative analyses of selective radiolabeled monoclonal antibody localization in metastatic lesions of colorectal cancer patients. Cancer Res 1987;47:1185–1189.
2. Bale WF, Contreras MA, Grady ED. Factors influencing localization of labeled antibodies in tumors. Cancer Res 1980;40:2965–2972.
3. Goldenberg DM, Goldenberg H, Sharkey RM, et al. Imaging of colorectal carcinoma with radiolabeled antibodies. Semin Nucl Med 1989;19:262–281.
4. Reilly RM. Immunoscintigraphy of tumors using ^{99m}Tc-labeled monoclonal antibodies: a review. Nucl Med Commun 1993;14:347–359.
5. Murray JL, Rosenblum MG, Lamki L, et al. Clinical parameters related to optimal tumor localization of indium-111-labeled mouse antimelanoma monoclonal antibody ZME-018. J Nucl Med 1987;28:25–33.

6. Divgi CR, Welt S, Kris M, et al. Phase I and imaging trial of indium-111-labeled anti-epidermal growth factor receptor monoclonal antibody 225 in patients with squamous cell lung carcinoma. *J Natl Cancer Inst* 1991;83:97–104.

7. Goldenberg DM, Goldenberg H, Sharkey RM, et al. Clinical studies of cancer radioimmunodetection with carcinoembrionic antigen monoclonal antibody fragments labeled with ^{123}I or [99m]Tc. *Cancer Res* 1990;50(suppl):909s–921s.

8. Hnatowich DJ, Griffin TW, Kosciuczyk C, et al. Pharmacokinetics of an indium-111-labeled monoclonal antibody in cancer patients. *J Nucl Med* 1985;26:849–858.

9. Hnatowich DJ, Gionet M, Rusckowski M, et al. Pharmacokinetics of ^{111}In-labeled OC-125 antibody in cancer patients compared with the 19-9 antibody. *Cancer Res* 1987;47:6111–6117.

10. Cohen S, Fava RA, Sawyer ST. Purification and characterization of epidermal growth factor receptor/protein kinase from normal mouse liver. *Proc Natl Acad Sci USA* 1982;79:6237–6241.

11. Cohen S, Ushiro N, Stoscheck C, Chinkers M. A native 170,000 epidermal growth factor receptor-kinase complex from shed plasma membrane vesicles. *J Biol Chem* 1982;257:1523–1531.

12. Pérez R, Pascual MR, Macias A, Lage A. Epidermal growth factor receptors in human breast cancer. *Breast Cancer Res Treat* 1984;4:189–193.

13. Rios MA, Fernández A, Tormo BR, et al. Heterogeneous expression of the EGF-receptor in human breast carcinoma. *Anticancer Res* 1992;12:205–208.

14. Neal DE, March C, Benett MK, et al. Epidermal growth factor receptors in human bladder cancer. Comparison of invasive and superficial tumors. *Lancet* 1985;1:346–348.

15. Magnusson I, Rosen AV, Nilsson R, Macias A, Pérez R, Skoog L. Receptors for epidermal growth factor and sex steroid hormones in human colorectal carcinomas. *Anticancer Res* 1989;9:299–302.

16. Veale D, Ashcroft T, March C, Gibson GJ, Harris AL. Epidermal growth factor receptors in non-small cell lung cancer. *Br J Cancer* 1987;55:513–516.

17. Snelling L, Miyamoto CT, Bender H, et al. Epidermal growth factor receptor 425 monoclonal antibodies radiolabeled with iodine-125 in the adjuvant treatment of high-grade astrocytomas. *Hybridoma* 1995;14:111–114.

18. Fernández A, Pérez R, Macias A, et al. Generation and primary characterization of the monoclonal antibodies against the epidermal growth factor receptor. *Interferón Biotecnología* 1989;6:289–299.

19. Fernández A, Spitzer E, Pérez R, et al. A new monoclonal antibody for detection of EGF-receptors in Western blots and paraffin-embedded tissue sections. *J Cell Biochem* 1992;49:157–165.

20. Rodríguez N, Torres O, Ramos M, et al. Immunogammagraphy with ^{99m}Tc-labeled mAb ior egf/r3 as a diagnostic tool of tumors of epithelial origin. [Abstract]. *Rev Esp Med Nucl* 1995;14:285.

21. Iznaga-Escobar N, Morales A, Núñez G. Micromethod for quantification of SH groups generated after reduction of monoclonal antibodies. *J Nucl Biol Med* 1996;23:641–644.

22. Throll JH, Freitas JE, Swanson D, Rogers WL, Clare JM. Clinical comparison of cardiac blood-pool visualization with ^{99m}Tc red blood cells in vivo and with ^{99m}Tc-human serum albumin. *J Nucl Med* 1976;19:796–803.

23. Macias A, Pérez R, Lage A. Estudios sobre el factor de crecimiento epidérmico (EGF) II: desarrollo de un radioreceptor analisis para la determinación de cantidades picomolares. *Interferón Biotecnología* 1985;2:115–127.

24. Akaike A. Posterior probabilities for choosing regression model. *Ann Inst Math Stat* 1978;30:A9–A14.

25. Jennrich RI, Sampson PF. Application of stepwise regression to nonlinear least squares estimation. *Techometrics* 1968;10:63–72.

26. Yamaoka K, Nakagawa T, Uno T. A nonlinear multiple regression program, MULT(2)(Bayes), based on a Baye(s) algorithm for microcomputers. *J Pharmacobio Dyn* 1978;8:246–256.

27. Yamaoka K, Nakagawa T, Uno T. Application of Akaike's information criterion (AIC) in the evaluation of linear pharmacokinetic equations. *J Pharmacokinet Biopharm* 1978;6:165–175.

28. Yamaoka K, Nakagawa T, Uno T. Statistical moments in pharmacokinetics. *J Pharmacokin Biopharm* 1978;6:547–558.

29. Gibaldi M, Perrier D. Pharmacokinetics. In: Gibaldi M, Perrier D, eds. *Pharmacokinetics*, 2nd ed. New York: Marcel Dekker; 1982:319–355.

30. Webster WB, Harwood SJ, Carroll RG, Morrissey MA. Pharmacokinetics of indium-111-labeled B72.3 monoclonal antibody in colorectal cancer patients. *J Nucl Med* 1992;33:498–504.

31. Wagner IG. *Fundamentals of clinical pharmacokinetics*. Hamilton, IL: Drug Intelligence; 1979;77–79.

32. Zuckier LS, Rodriguez LD, Scharff MD. Immunologic and pharmacologic concepts of monoclonal antibodies. *Semin Nucl Med* 1989;19:166–186.

33. Halpern SE, Hagan P. Effect of protein mass on the pharmacokinetics of murine monoclonal antibodies [Letter]. *J Nucl Med* 1985;26:818–819.

34. Carrasquillo JA, Abrams PG, Schroff RW, et al. Effect of antibody dose on the imaging and biodistribution of indium-111 9.2.27 anti-melanoma monoclonal antibody. *J Nucl Med* 1988;29:39–47.

35. Carrasquillo JA, Colcher D, Sugarbaker P, et al. Radioimmunoscintigraphy of colon cancer with iodine-131 labeled B72.3 monoclonal antibody. *J Nucl Med* 1988;29:1022–1030.

36. Carrasquillo JA, Bunn PA, Keenan AM, et al. Radioimmunodetection of cutaneous T cell lymphoma (CTCL) with 111-indium-labeled T101 monoclonal antibodies. *N Engl J Med* 1986;315:673–680.

37. de Bree R, Roos JC, Quak JJ, den Hollander W, Snow GB, Van Dongen GAMS. Radioimmunoscintigraphy and biodistribution of technetium-99m-labeled monoclonal antibody U36 in patients with head and neck cancer. *Clin Cancer Res* 1995;1:591–598.

38. Murray JL, Rosenblum M, Lamki L, et al. Imaging findings and pharmacokinetics of 111-indium ZM8–018 monoclonal antibody (MoAB) in malignant melanoma [Abstract]. *J Nucl Med* 1985;26:16.

39. Goldenberg DM, Deland FH. History and status of tumor imaging with radiolabeled antibodies. *J Biol Resp Modif* 1983;1:121–136.

40. Eger RR, Covell DG, Carrasquillo JA, et al. Kinetic model for the biodistribution of ^{111}In-labeled monoclonal antibody in humans. *Cancer Res* 1987;47:3328–3336.

41. Larson SM, Brown JP, Wright PW, et al. Imaging of melanoma with I-131-labeled monoclonal antibodies. *J Nucl Med* 1983;24:123–129.

42. Kirkwood JM, Neumann RD, Zoghbi SS, et al. Scintigraphic detection of metastatic melanoma using indium 111/DTPA conjugated anti-gp240 antibody (ZME-018). *J Clin Oncol* 1987;5:1247–1255.

43. Dean C, Modjtahedi H, Eccles S, Box G, Styles J. Immunotherapy with antibodies to EGF receptor. *Int J Cancer* 1994;8(suppl):103–107.

44. Modjtahedi H, Hickish T, Nicolson M, Moore J, Styles J, et al. Phase I trial and tumor localization of the anti-EGF-R monoclonal antibody ICR62 in head and neck or lung cancer. *Br J Cancer* 1996;73:228–235.

45. Brady LW, Miyamoto C, Woo DV, et al. Malignant astrocytomas treated with iodine-125 labeled monoclonal antibody 425 against epidermal growth factor receptor: a phase II trial. *Int J Radiat Oncol Biol Phys* 1992;22:225–230.

46. Dadparvar S, Krishna L, Miyamoto C, et al. Indium-111-labeled anti-EGFr-425 scintigraphy in the detection of malignant gliomas. *Cancer* 1994;73:884–889.

47. Miyamoto C, Brady LW, Rackover M, et al. Utilization of ^{125}I monoclonal antibody in the management of primary gliobastoma multiforme. *Radiol Oncol Invest* 1995;3:126–132.

48. Haunschild J, Steiner K, Faro HP, Senekowitsch R. Pharmacokinetics of reshaped MAb 425 in three animal species. *Cell Biophys* 1995;26:167–182.

49. Reilly RM, Kirsh J, Gallinger S, et al. Compartmental analysis of the pharmacokinetics of radioiodinated monoclonal antibody B72.3 in colon cancer patients. *J Nucl Biol Med* 1993;20:57–64.

50. Reilly RM, Sandhu J, Alvarez-Diez TM, et al. Problems of delivery of monoclonal antibodies. Pharmaceutical and pharmacokinetic solutions. *Clin Pharmacokinet* 1995;28:126–142.

51. Reynolds JC, Del Vecchio S, Sakahara H, et al. Anti-murine antibody response to mouse monoclonal antibodies: clinical findings and implications. *Int J Rad Appl Instrum [B]* 1989;16:121–125.

52. Mateo C, Moreno E, Amour K, Lombardero J, Harris W, Pérez R. Humanization of a mouse monoclonal antibody that blocks the epidermal growth factor receptor: recovery of antagonistic activity. *Immunotechnology* 1997;3:71–81.

53. Iznaga-Escobar N, Torres LA, Morales A, et al. Technetium-99m-labeled anti-EGF-receptor antibody in patients with tumor of epithelial origin: I. Biodistribution and dosimetry for radioimmunotherapy. *J Nucl Med* 1998;39:15–23.

54. Fritzberg AR, Beaumier PL. Targeted proteins for diagnostic imaging: does chemistry make a difference? [Editorial]. *J Nucl Med* 1992;33:394–397.